



2

30 continental site reflected shorter lifetime during the day, possibly because of photolysis of
31 some NPAHs. The yields of formation of 2NFLT and 2NPYR in marine air seem to be close
32 to the yields for OH-initiated photochemistry observed in laboratory experiments under high
33 NO_x conditions. Good agreement is found for prediction of NPAH gas-particle partitioning
34 using a multi-phase poly-parameter linear free energy relationship. Sorption to soot is found
35 less significant for gas-particle partitioning of NPAHs than for PAHs.

36 The NPAH levels determined in the southeastern outflow of Europe confirm intercontinental
37 transport potential.

38

39 **Keywords:** long-range transport potential, semi-volatile organic compounds, PAH
40 photochemistry,

41

42 1. Introduction

43 PAHs may undergo chemical transformations in the gaseous and in the particulate phase
44 (Finlayson-Pitts and Pitts, 2000; Keyte et al., 2013). Nitro-PAHs (NPAHs), earlier predicted
45 based on smog-chamber experiments (Atkinson and Arey, 1994), and later observed in urban
46 and rural areas (Finlayson-Pitts and Pitts, 2000; Keyte et al., 2013), seem to be most
47 significant derivatives: Mutagenicity and toxicity of atmospheric aerosols in general is mostly
48 related to NPAHs (Grosjean et al., 1983; Garner et al., 1986; Finlayson-Pitts and Pitts, 2000;
49 Claxton et al., 2004; Hayakawa, 2016). A large part, more than one third of the mutagen
50 potential of ambient may be attributable to NPAHs (Schuetzle, 1983).

51 Secondary formation of NPAH from PAHs is thought to occur on short time scales (hours).
52 This has been observed for PAHs collected on filters (Ringuet et al., 2012a; Zimmermann et
53 al., 2013; Jaryasopit et al., 2014a, 2014b), and also in in urban plumes (Bamford and Baker,
54 2003; Arey et al., 1989; Reisen and Arey, 2005). Although many NPAHs are emitted from
55 road traffic, only few are abundant in this source type (Arey, 1998; Keyte et al., 2013 and
56 2016; Inomata et al., 2015; Alves et al., 2016). The occurrence of various isomers of
57 nitrofluoranthene (NFLT) and nitropyrene (NPYR) can be used to study PAH sources, PAH
58 chemical transformations and the role of the photo-oxidants hydroxyl radical (OH) and nitrate
59 radical (NO₃) (Ciccioli et al., 1996; Finlayson-Pitts and Pitts 2000). E.g., 3- and 2-
60 nitrofluoranthene (3-, 2NFLT) are indicative for primary and secondary sources, respectively.



61 These substances have been suggested as tracers for air pollution on the time scales of hours
62 to days (Ciccioli et al., 1996; Finlayson-Pitts and Pitts 2000; Keyte et al. 2013).

63 Like their precursors, NPAHs are SVOCs, partitioning between the phases of the atmospheric
64 aerosol. Similar to other SVOCs, the NPAHs' phase distribution was found to depend on
65 temperature (summer and winter campaigns in the Alps; Albinet et al., 2008) and results from
66 both absorptive as well as adsorptive contributions (Tomaz et al., 2016). NPAHs have
67 primarily been observed in polluted areas (e.g. Pitts et al., 1985; Ramdahl et al., 1986; Garner
68 et al., 1986; Albinet et al., 2006 and 2008a; Ringuet et al., 2012a and 2012b; Zimmermann et
69 al., 2012; Barrado et al., 2013; Li et al., 2016). However, NPAHs have hardly been studied in
70 the unpolluted environment: Few studies were conducted in the rural environment i.e., in
71 Germany (Ciccioli et al., 1996), in the French Alps (100-1000 pg m⁻³ range for the sum of 10
72 NPAHs; Albinet et al., 2008) and in northern China (Li et al., 2016). Very few measurements
73 were performed in the remote atmospheric environment i.e., in the Mediterranean (Tsapakis
74 and Stephanou, 2007), in the Himalayas (single data; Ciccioli et al. 1996), and in the Arctic
75 (with so-called Arctic haze; Masclet et al. 1988; Halsall et al. 2001). With regard to the long-
76 range transport potential, the state of the knowledge is that at least some NPAHs are suspect
77 to go into intercontinental transport (Lafontaine et al., 2015) and might be ubiquitous in the
78 global atmosphere (Ciccioli et al., 1996).

79 However, a lack of NPAH data from remote atmospheric environments is obvious and little is
80 known about their long-range transport potential. The aim of this study was to study the long-
81 range transport potential of NPAHs by measurements at remote sites of Europe, addressing
82 the continental background and the outflow of the continent.

83

84 **2. Methodology**

85 **2.1 Sampling**

86 High-volume air sampling was conducted at a marine background site, Finokalia
87 (35.3°N/25.7°E, 250 m a.s.l.), in the context of a coordinated field experiment 2-13 July 2012
88 (Lammel et al., 2015) and at a continental background site in central Europe, K-pusztá
89 (46°58'N/19°33'E, 125 m a.s.l.; Degrendele et al., 2016), 5-16 August 2013. The Finokalia site
90 is located on a cliff at the northern coast of Crete, some 70 km east of major significant
91 anthropogenic emissions (Iraklion, a city of 100000 inhabitants with airport and industries;
92 Mihalopoulos et al., 1997; Kouvarakis et al., 2000). The K-pusztá site is located on a clearing,
93 characterised by uncultivated grassland, in a mostly coniferous forest in the Hungarian



4

94 (Pannonian) Great Plain, ca. 70 km and 270 km southeast of Budapest and Vienna,
95 respectively (≈ 2 mn inhabitants each). The background site character of both observatories
96 had been demonstrated (Borbély-Kiss et al., 1988; Kouvarakis et al., 2000; Vrekoussis et al.,
97 2005). Meteorological and trace gas measurements are covered by both observatories, which
98 are stations of the EMEP network (EMEP, 2015).

99 High volume air samples were collected using a HV-100P (Baghirra, Prague, Czech
100 Republic), equipped with a multi-stage cascade impactor (Andersen Instruments Inc.,
101 Fultonville, New York, USA, series 230, model 235) with five impactor stages, corresponding
102 to 10–7.2, 7.2–3, 3–1.5, 1.5–0.95 and 0.95–0.49 μm of aerodynamic particle size, D , (spaced
103 roughly equal $\Delta\log D$), a backup filter collecting particles $< 0.49 \mu\text{m}$ and, downstream, two
104 polyurethane foam plugs (PUFs, Molitan, Břeclav, Czech Republic, density 0.030 g cm^{-3} ,
105 placed in a glass cartridge), together 10 cm high. Particles were sampled on slotted QFF
106 substrates (TE-230-QZ, Tisch Environmental Inc., Cleves, USA, $14.3 \times 13.7 \text{ cm}$) and glass
107 fibre filters (Whatman, $20.3 \times 25.4 \text{ cm}$). The filters had been cleaned prior to use by heating
108 (330°C). PUFs were cleaned (8 hour-extraction in acetone and 8 hours in dichloromethane
109 (DCM)), wrapped in two layers of aluminum foil, placed into zip-lock polyethylene bags and
110 kept in the freezer prior to deployment. The sampler was operated at constant flow rate of 68
111 $\text{m}^3 \text{ h}^{-1}$. Day/night sampling (changing at sunset and sunrise) of gaseous samples (PUF) was
112 performed at both sites ($V = 600\text{--}1000 \text{ m}^3$), while at the marine site the impactor filter (QFF)
113 samples were collected over 24 h (5) or 48 h (3).

114 Particle number concentration was determined by an optical particle counter (Grimm model
115 107, Ainring, 31 channels between 0.25 and 32 μm of aerodynamic particle diameter, D).
116 Aerosol surface concentration, $S \text{ (cm}^{-1}\text{)}$, was derived as $S = \pi \sum_i N_i D_i^2$ assuming sphericity.
117 Hereby, true S will be underestimated, in particular if particles of irregular form were
118 abundant (e.g. Jaenicke, 1988). Comparisons with absolute methods (e.g. Pandis, et al. 1991)
119 suggest that the discrepancy may reach up to a factor of 2-3. The mass median diameter (D_m ,
120 μm), was derived as $\log D_m = \sum_i m_i \log D_i / \sum_i m_i$ with m_i denoting the mass in size class i , D_i
121 being the geometric mean diameter collected on stage i of the cascade impactor.

122

123 2.2 Chemical analysis

124 All air samples were extracted with DCM using an automatic warm Soxhlet extractor (Büchi
125 B-811, Switzerland). Deuterated PAHs (D8-naphthalene, D10-phenanthrene, D12-perylene;



126 Wellington Laboratories, Canada) were used as surrogate standards for both PAHs and
127 NPAHs. These were spiked on each PUF prior to extraction. The extract was split in two
128 parts, 1/9 for PAHs and Nitro-PAHs analysis, 9/10 for PBDEs, PCBs and OCPs. The PAHs
129 and Nitro-PAHs aliquot was a subject to open column chromatography clean-up. Glass
130 column (1 cm i.d.) was filled with 5 g activated silica (150°C for 12 h), sample was loaded
131 and eluted with 10 mL *n*-hexane, followed by 40 mL DCM. The cleaned sample was
132 evaporated under a stream of nitrogen in a TurboVap II apparatus (Biotage, Sweden),
133 transferred into a conical GC vial and spiked with recovery standard, terphenyl, the volume
134 was reduced to 100 µL.

135 GC-MS analysis of 4-ring PAHs (fluoranthene (FLT), pyrene (PYR), benzo(b)fluorene
136 (BBN), benzo(a)anthracene (BAA), triphenylene (TPH) and chrysene (CHR)) and 2-4 ring
137 NPAHs (1- and 2-nitronaphthalin (1-, 2NNAP), 3- and 5-nitroacenaphthene (3-, 5NACE), 2-
138 nitrofluorene (2NFLN), 9-nitroanthracen (9NANT), 3- and 9-nitrophenanthren (3-, 9NPHE),
139 2- and 3-nitrofluoranthene (2-, 3NFLT), 1- and 2-nitropyrene (1-, 2NPYR), 7-
140 nitrobenz(a)anthracene (7NBAA), 6-nitrochrysene (6NCHR) was performed using a gas
141 chromatograph atmospheric pressure chemical ionization tandem mass spectrometer (GC-
142 APCI-MS/MS) instrument, Agilent 7890A GC (Agilent, USA), equipped with a 60m ×
143 0.25mm × 0.25µm DB-5MSUI column (Agilent, J&W, USA), coupled to Waters Xevo TQ-S
144 (Waters, UK). Injection was 1 µL splitless at 280°C, with He as carrier gas at constant flow
145 1.5 mL min⁻¹. The GC oven temperature program was as follows: 90°C (1 min), 40°C/min
146 to 150°C, 5°C/min to 250°C (5 min) and 10°C/min to 320°C (5 min). APCI was used in
147 charge transfer conditions. The isomers 2- and 3NFLT were not separated by the GC method,
148 but co-eluted and are reported as sum.

149 Recovery of native analytes varied 72-102% for PAHs and deuterated PAHs, 70-110% for
150 NPAHs (details see supplementary material (SM), Table S1a). The results were not recovery
151 corrected. The mean of field blank values was subtracted from the sample values. Values
152 below the mean + 3 standard deviations of the field blank values were considered to be
153 <LOQ. 3 field blanks of the sampling media types (slotted and backup QFF, PUF) were
154 collected at each site. Field blank values (listed in SM, Table 1c) of some analytes were below
155 the instrument limit of quantification (ILOQ), which corresponded to 0.004-0.069 pg m⁻³ for
156 NPAHs (except for 1NNAP for which it ranged 0.60-0.87 pg m⁻³) and 0.010-0.126 pg m⁻³ for
157 4-ring PAHs (except for FLT and PYR for which it ranged 0.17-0.59 pg m⁻³) (Table S1b).



6

158 Higher LOQs were determined for some of the NPAHs and for all 4-ring PAHs in gaseous air
159 samples (PUFs), namely 0.006-0.009 ng (corresponding to 3.5-8.0 pg m^{-3}) for 3NACE and
160 2NPYR, 0.028-0.097 (corresponding to 16-86 pg m^{-3}) for 2NNAP, 2NFLT and 1NPYR, and
161 0.10-0.27 ng (corresponding to ≈ 60 -240 pg m^{-3}) for 4-ring PAHs (except for FLT and PYR for
162 which it was 1.71 and 1.05 ng, respectively, corresponding to ≈ 600 -1500 pg m^{-3}). In
163 particulate phase samples, where separate field blanks for the 2 different QFFs were
164 determined (on the impactor stages on one hand side and the backup filter on the other hand
165 side, Tbalc S1c), higher LOQs were determined for some of the NPAHs and for all 4-ring
166 PAHs, namely 0.008-0.089 ng (corresponding to 4.6-79 pg m^{-3}) for 2NNAP, 2NFLT, 1NPYR
167 and 2NPYR, 0.26-0.31 ng (corresponding to 150-274 pg m^{-3}) for 9NANT, and 0.05-0.22 ng
168 (corresponding to ≈ 30 -200 pg m^{-3}) for 4-ring PAHs (except for FLT and PYR for which it was
169 0.79 and 0.36 ng, respectively, corresponding to ≈ 200 -700 pg m^{-3}).

170 The breakthrough in PUF samples was estimated (Pankow, 1989; ACD, 2015; Melymuk et
171 al., 2016), and as a consequence, 2-3 ring PAHs and 2-ring NPAHs results were excluded
172 from this study as their sampling may have been incomplete. We, therefore, report $\Sigma_6 4\text{rPAH}$
173 and $\Sigma_{11} 3\text{-4rNPAH}$.

174 Particulate matter mass (PM_{10}) was determined by gravimetry, and organic matter (OM) and
175 elemental carbon (EC) contents of PM by a thermal-optical method (Sunset Lab., USA;
176 EUSAAR protocol).

177

178 2.3 Gas-particle partitioning

179 Gas-particle partitioning was studied by applying a multiphase ppLFFER model, which was
180 recently introduced (Shahpoury et al., 2016). In brief, partitioning of semivolatile compounds
181 in air can be described (Yamasaki et al., 1982), by

182

$$183 K_p = c_{ip} / (c_{ig} \times c_{PM})$$

184

185 where K_p ($\text{m}^3 \text{air} (\text{g PM})^{-1}$) is the temperature dependent partitioning coefficient, c_{PM} (g m^{-3}) is
186 the concentration of particulate matter in air, c_{ip} and c_{ig} are the analyte (i) concentrations (ng
187 m^{-3}) in the particulate and gas phase, respectively. K_p can be predicted using models based on
188 single- and poly-parameter linear free energy relationships (spLFFER, ppLFFER). spLFFER's
189 relate the partitioning coefficient to one physic-chemical property i.e., assume one process to



7

190 determine the sorption process, while ppLFER's in principle account for all types of
191 molecular interactions between solute and matrix (Goss and Schwarzenbach, 2001). The
192 observed particulate mass fractions were tested with both a spLFER and a ppLFER model.
193 The spLFER chosen is the widely used K_{oa} model of Finizio et al., 1997 (results presented in
194 the SM, S2.3). The ppLFER is a multi-phase model recently presented (Shahpoury et al.,
195 2016) and applied for NPAHs (Tomaz et al., 2016). It is based on linear solvation energy
196 relationships (Abraham, 1993; Goss, 2005):

197

$$198 \log K_p = eE + sS + aA + bB + lL + c$$

$$199 \log K_p = sS + aA + bB + vV + lL + c$$

200

201 where capital letters E, S, A, B, L, and V are solute-specific Abraham solvation parameters for
202 excess molar refraction (describes interactions between π - and lone (n-) electron pairs),
203 polarizability/ dipolarity, solute H-bond acidity, solute H-bond basicity, logarithm of solute
204 hexadecane-air partitioning coefficient (unitless), and McGowan molar volume (cm^3
205 mol^{-1})/100, respectively (Endo and Goss, 2014). The corresponding parameters e, s, a, b, l,
206 and v reflect matrix-specific solute-independent contribution to K_p . In lack of experimental
207 data, the solute descriptors for NPAHs were taken from M.H. Abraham (personal
208 communication). The multi-phase ppLFER considers adsorption onto soot, $(\text{NH}_4)_2\text{SO}_4$, and
209 NH_4Cl , and absorption into OM. OM is assumed to be constituted of two separate phases, low
210 to high molecular mass, both organic and water soluble OM, represented by a ppLFER
211 equation for dimethyl sulfoxide-air on one hand side, and high molecular mass OM,
212 represented by a ppLFER equation for polyurethane ether-air (Shahpoury et al., 2016).

213 A conventional single-parameter LFER (K_{oa}) model is applied, too.

214

215 **2.4 Air mass history analysis**

216 The HYSPLIT (Draxler and Rolph, 2003) and FLEXPART (Stohl et al., 1998, 2005) models
217 were used to identify air mass histories over 10 and 2 days, respectively. The possible
218 influence of polluted air on samples was quantified using a novel method of applying
219 Lagrangian particle statistics (FLEXPART, see SM, S2.2). To this end, for the entire sampling
220 period, one particle per second was released. The model output is generated at 0.062° (≈ 7
221 km), every 30 minutes and expressed as 'residence time' i.e., a measure of the time particles



8

222 resided in grid cells. ECMWF meteorological data ($0.125^\circ \times 0.125^\circ$ resolution, hourly) were
223 used as input.

224

225 3. Results and discussion

226 The NPAH levels are distinctly lower at the marine than at the continental site, $\sum_{11\ 3-4r}$ NPAH =
227 22.5 and 58.5 pg m^{-3} , respectively (Table 1). The NPAHs showing the highest concentrations
228 were 2NFLT and 3NPHE at the marine (Fig. 1b) and 9NANT and 2NFLT at the continental
229 site (Fig. 1d, Table 2). The substance patterns at both sites are similar, though ($R^2 = 0.76$, $P >$
230 0.99 , t-test). At the marine site, advection was northerly, with air masses originating (time
231 horizon 10 days) in eastern and central Europe and, towards the end of the campaign, in the
232 western Mediterranean. The site was placed into the southeastern outflow of Europe. NO_x
233 ($0.2\text{-}0.6$ ppbv), EC ($0.2\text{-}0.8$ $\mu\text{g m}^{-3}$) and PM_{10} ($18.3\text{-}39.3$ $\mu\text{g m}^{-3}$) reflect background
234 conditions. Air mass history analysis suggests that the somewhat elevated concentration in the
235 first sample collected at the marine site (Fig. 1a) is related to long-range transport influenced
236 by passage over the urban areas of Izmir and Istanbul (urban fractional dose $D_u = 5.0\%$, in
237 contrast to the mean which was 1.6%; Fig. S3). Overall, urban fractional dose in the range
238 $<0.002\text{-}5.4\%$ was received at the marine site. Across all samples at the marine site, D_u is
239 found to be significantly correlated with the pollutant sum concentrations $\sum_{6\ 4r}$ PAH and $\sum_{11\ 3-}$
240 $_{4r}$ NPAH ($R^2 = 0.61$ and 0.69 , respectively, both $P > 0.99$).

241 From this data set, subsets of each two samples are formed, representing minimum (i.e.,
242 almost no influence from industrialised area 48 hours prior to arrival (hereforth called ‘marine
243 background’, urban fractional dose $D_u = 0.4\%$) and maximum observed influence (hereforth
244 called ‘background with urban influence’, $D_u = 3.1\%$; SM Table S2, Figure S3). The results
245 for these subsets are listed in Tables 1-3. Such classification was not deemed meaningful for
246 the samples collected at the continental site, as the relevant source distribution in central
247 Europe was too homogeneous during this episode. Advection was mostly from northwest and
248 partly from easterly directions, with air mass origin (time horizon of 10 days) mostly in central
249 Europe and, to a lesser extent in eastern Europe and the western Balkans. The NO_2 ($1.2\text{-}2.6$
250 ppbv), total carbon ($3\text{-}6$ $\mu\text{g m}^{-3}$) and PM_{10} ($10.7\text{-}46.3$ $\mu\text{g m}^{-3}$) levels during the campaign
251 reflect continental background conditions.

252 The 4-ring PAH concentrations in samples from the continental site on the one hand, and in
253 background air with urban influence collected at the marine site (urban areas 300-500 km



9

254 away) on the other hand, are similar (Table 2). Also, the substance patterns are more similar
255 than when relating all samples at the marine site i.e., $R^2 = 0.88$ ($P > 0.999$, t-test) instead of R^2
256 $= 0.76$. At both sites, 4rPAHs were in fact influenced by secondary emissions, namely
257 throughout day and night from the soil (by average 16.3 and $9.3 \text{ pg m}^{-2} \text{ h}^{-1}$ for FLT and PYR,
258 respectively; Degrendele et al., 2016) or occasionally from surface seawater (during at least 1
259 day-time interval out of in total 3 of this data subset; Lammel et al., 2016). In the data set from
260 the continental site, we study day/night (D/N) effects (subsets listed in Tables 1-3, too): PAH
261 concentrations were $\approx 60\%$ higher during the day than during the night, while NPAH
262 concentrations were by average $\approx 5\%$ lower during the day. PAH concentrations were driven
263 by re-volatilisation from soil, determined by temperature variation (Degrendele et al., 2016).
264 For NPAHs (partly primary emitted) this indicates that the higher emissions during the day
265 (due to re-volatilisation and road traffic) were compensated by lower lifetime (because of
266 heterogeneous photolysis; Fan et al., 1996; Feilberg and Nielsen, 2000, 2001; García-Berriós
267 et al., 2017). The same could be reflected in different NPAH/PAH ratios (the potential NPAH
268 yields), which were 5.6% and 8.9% at the marine and continental sites, respectively. These
269 were influenced by similar substance patterns upon emission, similar irradiation (summer, no
270 or almost no clouds) and deposition velocities (θ in the range 0.05-0.20 for $\Sigma_{11} 3\text{-}4\text{rNPAH}$ and
271 $\Sigma_6 4\text{rPAH}$, no precipitation), but different re-volatilisation fluxes and different characteristic
272 transport times elapsed. Distance to major urban source areas was 300- >1000 km at the
273 marine and 100-500 km at the continental site. The NPAH/PAH ratios being lower at the
274 more distant receptor site, the marine site, may suggest that photochemical degradation of
275 NPAHs along transport was on average faster than degradation of the precursors.

276

277 The NPAH levels observed in marine background air are the lowest ever reported.
278 Remarkably, the concentrations are much lower, by more than one order of magnitude, than
279 one decade before at the same site during the same season (Tsapakis and Stephanou, 2007).
280 The concentrations observed now are a factor of 4-10 lower than in a forest site in Amazonia
281 two decades before (which might have been influenced by biomass burning emissions), and
282 also a factor of 3 lower (for 2NPYR) than observed at an extremely remote site in the
283 Himalayas two decades before (Ciccioli et al., 1996; Table 3). The NPAH levels observed at
284 the marine site with influence of pollution and at the continental site are comparable, but also



10

285 at the lower end of the range spanned by previous observations at rural and remote sites
286 (Table 3).

287

288 **Gas-particle partitioning**

289 The time-weighted mean NPAH phase distributions ($\Sigma_{113-4rNPAH}$) differ, corresponding to θ
290 = 0.05 and 0.17 at the marine and continental sites, respectively, – despite similar
291 temperatures (Table 1). In contrast and despite of similar temperature ranges, the 4-ring
292 PAHs' (Σ_64rPAH) particulate mass fraction was higher at the marine than at the continental
293 site ($\theta = 0.42$ and 0.20 , respectively). The NPAH mass size distribution had its maximum in
294 the $<0.49 \mu\text{m}$ size range at both sites. The 4-ring PAHs mass size distribution had 2 maxima,
295 $<0.49 \mu\text{m}$ and between 0.95 and $1.5 \mu\text{m}$, at the marine site, but one at $<0.49 \mu\text{m}$ at the
296 continental site (Table 1). This is probably related to the presence of aged aerosol at the
297 marine site vs. a larger contribution of fresh aerosols at the continental site. This is,
298 furthermore, supported by the analysis of air mass origins that shows significant influence of
299 urban areas for only few samples at the marine and for all samples at the continental site (SM
300 S2).

301 Both 4-ring PAHs and 3-4 ring NPAHs were more associated with PM in polluted air than in
302 clean air. This trend is weak for PAHs with $\theta = 0.02$ for Σ_64rPAH in marine background but
303 0.07 in background with urban influence (and $\theta = 0.09$ and 0.25 for CHR; Table 2), but is
304 obviously strong for NPAHs, namely $\theta = 0.19$ for 2NPYR in marine background but 0.70 in
305 background with urban influence, ≈ 0.93 in polluted continental air, and $\theta = 0.01$ for Σ_{113-}
306 $4rNPAH$ in marine background but 0.21 in background with urban influence (Table 2). The
307 urban influenced air at the marine site is also reflected in a much higher OC (a factor of 3
308 higher than the all-campaign mean) and elevated EC, (less prominent, $\approx 50\%$ above mean).
309 This confirms the understanding that gas-particle partitioning of both PAHs (Lohmann and
310 Lammel, 2004; Shahpoury et al., 2016) and NPAHs (Tomaz et al., 2016) is mostly determined
311 by absorption in POM and adsorption to soot. When comparing polluted air at the continental
312 site and background with urban influence at the marine site, a strong shift of Σ_64rPAH
313 towards the particulate phase, $\theta \approx 0.21$ vs. 0.07 , respectively, is found, while for $\Sigma_{113-4rNPAH}$
314 θ are similar i.e., ≈ 0.16 vs. 0.21 , respectively. This phase partitioning trend of the 4rPAHs
315 could be explained by sorption to EC, which is a factor of ≈ 2 higher, but not by OC (only



316 $\approx 20\%$ higher). In conclusion, these observations consistently indicate that sorption to soot is
317 less significant for gas-particle partitioning of NPAHs than for PAHs.

318 While NPAHs were significantly phase-shifted ($\theta = 0.24$ during day-time but $\theta = 0.58$ during
319 night-time), this was not the case for 4rPAHs ($\theta = 0.18$ during day-time and $\theta = 0.23$ during
320 night-time). This is in line with the perception that the temperature sensitivity of phase change
321 is stronger for the substance class with stronger molecular interactions in the condensed phase,
322 NPAHs. E.g., the enthalpies of phase change between air and OC of FLT and NFLT are -98
323 and -75 kJ mol^{-1} , respectively (OC represented by DMSO; ACD, 2015).

324 Good agreement is found for the prediction of NPAH partitioning using the multi-phase (3-
325 phase) ppLFFER with most values predicted within one order of magnitude of the observed
326 values (Fig. 2; quantification of deviations in S2.3.1). The agreement is better than assuming
327 absorption (into OM) to be the only relevant process (K_{oa} model; see S2.3.2, Fig. S5). The
328 same was found when studying gas-particle partitioning of NPAHs in urban air (Tomaz et al.,
329 2016). This supports the perception that gas-particle partitioning of NPAHs is governed by
330 various molecular interactions with OM, with its polarity being well represented by DMSO,
331 better than by octanol. Earlier, it had been found for eight 3-4rNPAHs at urban and rural sites
332 (Li et al., 2016) that the dual model, assuming adsorption (to soot) and absorption (into OM)
333 predicts better than single adsorption (to the total aerosol surface i.e., Junge-Pankow) or single
334 absorption (K_{oa}) models do.

335 The interactions with the aerosol matrix of 9NPHE (continental site) and 5NACE, 2NFLN,
336 2NFLT and 1NPYR (marine site) are less well represented than other NPAHs by the model as
337 suggested by low slopes of their $\log K_p \text{ experimental} / \log K_p \text{ predicted}$ relationships. Further
338 conclusions are not supported by the limited amount of data and uncertainties on both the
339 model (estimated ppLFFER parameters) and experimental (concentrations close to LOQ) sides.

340

341 **Mass size distributions**

342 Sums of NPAHs' and PAHs' mass size distributions are found unimodal with the maximum
343 in particles $< 0.49 \mu\text{m}$, except PAHs at the marine site, which shows a second maximum
344 between 1.5 and $3.0 \mu\text{m}$ (Fig. 3). At the marine site, 50 and 69% of 1NPYR and 2NFLT,
345 respectively, were found associated with particles $< 0.45 \mu\text{m}$ and 68 and 86%, respectively,
346 with particles $< 0.95 \mu\text{m}$, and even more, 83% and 100%, respectively, with particles $< 0.45 \mu\text{m}$
347 at the continental site.



12

348 Σ_6 4rPAH mass size distributions are shifted to larger particles in background with urban
349 influence as compared to marine background air (both collected at the marine site) i.e., MMD
350 = 0.19 and 0.28, respectively. However, such a trend is not apparent for NPAHs (Table 2). The
351 size shift of PAHs is not corresponding to the PM_{10} mass size distribution: The MMD of PM_{10}
352 for all samples collected at the marine site was 0.58 μm , while it was 1.13 and 0.62 μm in the
353 marine background and background with urban influence data subsets, respectively. The PM_{10}
354 as well as the OC mass size distributions were bimodal with maxima corresponding to < 0.49
355 μm and 3.0-7.2 μm particles (MMDs listed in Table 2), while the EC mass size distribution
356 was unimodal, with the maximum concentration in the finest fraction. At the continental site,
357 the Σ_{11} 3-4rNPAH mass size distribution was bimodal with maxima corresponding to < 0.49
358 μm and 7.2-10 μm particles, while the Σ_6 4rPAH mass size distribution was unimodal, with the
359 maximum concentration in the finest fraction (for all samples as well as for day and night data
360 subsets; Table 1).

361 The formation of a second maximum, at larger particles than emitted, reflects the
362 redistribution of semivolatile organics in an aged aerosol, hence, is expected at receptor sites
363 such as the marine site. This was also observed in polluted air, at rural and suburban sites, but
364 not at traffic sites or in winter at a rural site, when primary emissions dominated (unimodal;
365 Albinet et al., 2008b; Ringuet et al., 2012b).

366

367 **Substance patterns and NPAH formation during long-range atmospheric transport**

368 Among the targeted NPAHs and apart from NNAPs, which were highest concentrated,
369 2NFLT and 3NPHE prevailed at the marine site (accounting together for $\approx 60\%$ of the NPAH
370 mass, excluding the NNAPs), while at the continental site 9NANT and 2NFLT prevailed
371 (accounting for $\approx 65\%$ together) (Fig. 1, summarised in Fig. S4). The analytical method did not
372 separate the isomers 2NFLT and 3NFLT, but at receptor sites, far from diesel emissions it
373 appears justified to assume $c_{2NFLT} \gg c_{3NFLT}$ (Finlayson-Pitts and Pitts, 2000; Zimmermann et
374 al., 2012). The ratio 1NPYR/2NPYR is higher, ≈ 1 , at the continental site than at the marine
375 site (≈ 0.25), which reflects the significance of primary sources for polluted air (Atkinson and
376 Arey, 1994; Finlayson-Pitts and Pitts, 2000; Zimmermann et al., 2012). This ratio was found
377 similarly high or even higher at urban sites (Ringuet et al., 2012c; Tomaz et al., 2016).
378 Similarly, the ratio 2NFLT/1PYR, the concentration of a secondarily formed over a primary
379 emitted NPAH, has been used as indicator for fresh emissions (if < 5) vs. photochemically



380 aged air mass (Keyte et al., 2013). These values were $\gg 5$ in 21 out of 22 and 7 out of 8
381 samples at the marine and continental sites, respectively. The only sample collected at the
382 continental site with elevated primary NPAH ($2NFLT/1NPYR = 4.3$) was possibly influenced
383 by emissions from Budapest, which was passed by the advected air within the last hours
384 before arrival. The only sample collected at the marine site with elevated primary NPAH
385 ($2NFLT/1NPYR = 5.9$) was indeed directly influenced by emissions into the boundary layer
386 above the Izmir and Istanbul metropolitan areas (urban fractional dose $D_u = 5.0\%$ for samples
387 no. 1 and 2 in Fig. S3). In conclusion, these results from receptor / background sites confirm
388 the existing knowledge about primary emitted and secondarily formed NPAHs.

389 The ratio of two secondarily formed NPAHs, $2NFLT/2NPYR$, is indicative for day- vs. night-
390 time formation paths (Atkinson and Arey, 1994; Ciccioli et al., 1996) is found ≈ 2 at the
391 marine and ≈ 8 at the continental site (normalised to the precursor ratio i.e.,
392 $2NFLT/2NPYR/(FLT/PYR)$; Table 4). Such low values point to day-time (OH initiated)
393 formation, while night-time (NO_3 initiated) formation was negligible, practically excluded at
394 the marine site. This is in line with the perception that NO_3 must have been very low in this
395 remote environment. (NO_x levels at the marine site were in the range 0.2-0.6 ppbv). A similar
396 conclusion had been drawn in a semi-rural environment (Feilberg et al., 2001).

397 For $2NFLT$ and $2NPYR$ (secondary sources only) and for $1NPYR$, which has mostly primary
398 sources (Finlayson-Pitts and Pitts, 2000; Ringuet et al., 2012a; Jariyasopit et al., 2014a,
399 2014b) we infer the potential yields (Table 4). Here, yield is defined as c_{NPAH}/c_{PAH} (total
400 concentrations) and reflects an upper estimate, as other PAH photochemical sinks, such as
401 formation of oxy-PAHs, are neglected. The yield of $2NFLT$ in polluted air exceeds the one in
402 background air only slightly, while the yield of $2NPYR$ in polluted air exceeds the one in
403 background air much more (a factor of 3 higher).

404 As expected, the highest potential yield of $1NPYR$ is found in polluted air (both sites),
405 reflecting the dominance of primary emissions of $1NPYR$. Similarly, higher yields of
406 secondary NPAHs are found for marine background air compared to background air with
407 urban influence (marine site), reflecting the longer reaction times elapsed since PAH
408 emission. The yield for $2NFLT$, c_{2NFLT}/c_{FLT} , $\approx 2-4\%$ at both sites ranges higher than the one
409 for $2NPYR$, c_{2NPYR}/c_{PYR} , which is found $\approx 0.5-2\%$. Note that because of the co-elution of
410 $2NFLT$ and $3NFLT$, and neglect of $3NFLT$, the so derived values of c_{2NFLT}/c_{FLT} represent
411 actually upper estimates. Apart from sites which were immediately influenced by PAH sources



412 (road traffic, power plant, biomass burning), only very few studies reported NPAH together
413 with precursor data in both phases of ambient air. $c_{2\text{NPYR}}/c_{\text{PYR}} = 1.0\%$, similar to our finding at
414 remote sites, but a very high $c_{2\text{NFLT}}/c_{\text{FLT}} = 12.9\%$ were reported from a suburban site in France
415 in summer during day-time (corresponding values for night-time were 2.0 and 9.4%,
416 respectively; Ringuet et al., 2012c). 2NFLT was not separated from 3NFLT (similar to our
417 data set). A suburban site will be influenced by direct 3NFLT emissions, such that $c_{2\text{NFLT}}/c_{\text{FLT}}$
418 is an upper estimate. Much lower ratios, $c_{2\text{NFLT}}/c_{\text{FLT}} = 0.20\%$ and $c_{2\text{NPYR}}/c_{\text{PYR}} = 0.08\%$ were
419 reported as the median values for 90 sites of various categories, rural and urban, in northern
420 China in summer (Lin et al., 2015). These yields are somewhat higher for the subset of the
421 rural sites. The potential yields found at the marine site in our study are close to the yields for
422 OH-initiated photochemistry observed in laboratory experiments under high NO_x conditions
423 i.e., 3% for $c_{2\text{NFLT}}/c_{\text{FLT}}$ and 0.5% for $c_{2\text{NPYR}}/c_{\text{PYR}}$ (Atkinson and Arey, 1994).

424

425 4. Conclusions

426 For the first time pollution contained in individual background air samples was quantified, by
427 means of a fractional dose. The fractional dose indicated how much the collected volume of
428 air had been exposed to an urban boundary layer within a given time horizon. This is found
429 suitable to discriminate among samples and discuss results, clearly beyond qualitative
430 reasoning on back trajectories alone. The concept could be applied to any type of
431 georeferenced origin and might be useful to track the influence of land use of various kind, or
432 ship and aircraft routes.

433 Our measurements confirmed occurrence of mutagenic NPAHs, earlier reported from polluted
434 atmospheric environments of America, Europe and Asia, also for the European background
435 atmosphere and the outflow of Europe. These substances obviously go into intercontinental
436 transport and might be indeed ubiquitous. The long-range transport potential is hardly limited
437 by the mass size distribution, which is determined by the particle size upon emission (primary
438 NPAHs) and condensation and redistribution in the aerosol along transport, hence, does not
439 include the short-lived coarse mass fraction. However, the observation of 3.8 and 0.92 pg m^{-3}
440 of 2NFLT and 2NPYR, respectively, measured at the southeastern outflow of Europe (the
441 lowest ever reported concentrations; Table 3), may indicate that their abundance in the remote
442 global environment could be less than anticipated. Earlier, this was based on a single
443 measurement of 2NPYR, 3 pg m^{-3} , at an extremely remote site in central Asia two decades



15

444 before (Ciccioli et al., 1996). Moreover, this air, classified as marine background, was not
445 completely clean, but had been exposed to a non-zero fractional urban pollution dose (0.4% of
446 the total, time horizon of 2 days). More measurements at remote sites should verify levels
447 globally. PAHs have been abated significantly in Europe during the last decades (EEA, 2014),
448 which should also be reflected in long-term trends of their derivatives. However, a temporal
449 trend for the Aegean or the southeastern outflow of Europe in summer cannot be inferred
450 based on the current and the earlier (2002; Tsapakis and Stephanou, 2007) campaign data.
451 NPAHs should be included in monitoring programmes to better assess the exposure of human
452 health hazards of atmospheric pollution, even in remote areas.

453 Understanding of NPAH formation in ambient air is still rudimentary. Although our
454 observations of a potential NPAH yield are in agreement with laboratory studies of OH-
455 initiated photochemistry, the kinetics of NPAHs, both formation from parent PAHs and
456 photolysis remains to be quantitatively studied under relevant conditions for the background
457 atmosphere i.e., low NO_x and on various aerosol matrices including sea salt, respectively.

458

459 **Acknowledgements**

460 We thank Christos I. Efstathiou (Masaryk University), András Hoffer, Gyula Kiss (MTA-PE
461 Air Chemistry Research Group, Veszprém), Jiří Kohoutek (MU), Giorgos Kouvarakis
462 (University of Crete, Iraklion) and Lajos Szöke (Hungarian Meteorological Service) for on-
463 site support, Giorgos Kouvarakis and Krisztina Labancz (Hungarian Meteorological Service)
464 for meteorological and trace gas data, Michael H. Abraham (University College London) for
465 providing pPLFER solute descriptors, Ignacio Pisso (NILU, Kjeller, Norway) for model post-
466 processing scripts and Céline Degrendele (MU) and Manolis Tsapakis (Hellenic Centre for
467 Marine Research, Gournes) for discussion. This research was supported by the Czech Science
468 Foundation (n° P503 16-11537S), the Czech Ministry of Education, Youth and Sports (n°
469 LO1214 and LM2015051), and the European Union FP7 (n° 262254, ACTRIS).

470

471 **Compliance with Ethical Standards** No potential conflicts of interest (financial or non-
472 financial) exist.

473 **References**

- 474 Abraham, M.H.: Scales of solute hydrogen-bonding: their construction and application to physicochemical and
475 biochemical processes. *Chem. Soc. Rev.*, 22, 73–83, 1993.
- 476 ACD: ACD/Labs Absolv Software, Advanced Chemistry Development, Toronto, Canada, 2015.
- 477 Albinet, A., Leoz-Garziandia, E., Budzinski, H., and Villenave, E.: Simultaneous analysis of oxygenated and
478 nitrated polycyclic aromatic hydrocarbons on standard reference material 1649a (urban dust) and on natural
479 ambient air samples by gas chromatography-mass spectrometry with negative ion chemical ionisation. *J.*
480 *Chrom. A*, 1121, 106-113, 2006.



- 481 Albinet, A., Leoz-Garziandia, E., Budzinski, H., and Villenave, E.: Polycyclic aromatic hydrocarbons (PAHs),
482 nitrated PAHs and oxygenated PAHs in ambient air of the Marseille area (South of France): Concentrations
483 and sources. *Sci. Total Environ.*, 384, 280-292, 2007.
- 484 Albinet, A., Leoz-Garziandia, E., Budzinski, H., Villenave, E., and Jaffrezo, J.L.: Nitrated and oxygenated
485 derivatives of polycyclic aromatic hydrocarbons in the ambient air of two French alpine valleys part 1:
486 concentrations, sources and gas/particle partitioning. *Atmos. Environ.*, 42, 43-54, 2008a.
- 487 Albinet, A., Leoz-Garziandia, E., Budzinski, H., Villenave, E., and Jaffrezo, J.L.: Nitrated and oxygenated
488 derivatives of polycyclic aromatic hydrocarbons in the ambient air of two French alpine valleys part 2: Particle
489 size distribution. *Atmos. Environ.*, 42, 55-64, 2008b.
- 490 Alves, C.A., Vicente, A.M.P., Gomes, J., Nunes, T., Duarte, M., and Bandowe, B.A.M.: Polycyclic aromatic
491 hydrocarbons (PAHs) and their derivatives (oxygenated-PAHs, nitrated-PAHs and azaarenes) in size-
492 fractionated particles emitted in an urban road tunnel. *Atmos. Res.*, 180, 128-137, 2016.
- 493 Arey, J.: Atmospheric reactions of PAHs including formation of nitro-arenes. In: *The handbook of*
494 *Environmental Chemistry, Vol. 3I: PAHs and Related Compounds* (Neilson AH, ed.), Springer, Berlin, pp.
495 347-385, 1998.
- 496 Arey, J., Atkinson, R., Zielinska, B., and McElroy, P.A.: Diurnal concentrations of volatile polycyclic aromatic
497 hydrocarbons and nitroarenes during a photochemical air pollution episode in Glendora, California. *Environ.*
498 *Sci. Technol.*, 23, 321-327, 1989.
- 499 Atkinson, R., and Arey, J.: Atmospheric chemistry of polycyclic aromatic hydrocarbons: Formation of
500 atmospheric mutagens. *Environ. Health Persp.*, 102, 117-126, 1994.
- 501 Bamford, H.A., and Baker, J.E.: Nitro-polycyclic aromatic hydrocarbon concentrations and sources in urban and
502 suburban atmospheres of the Mid-Atlantic region. *Atmos. Environ.*, 37, 2077-2091, 2003.
- 503 Barrado, A.I., García, S., Sevillano, M.L., Rodríguez, J.A., and Barrado, E.: Vapor-phase concentrations of
504 PAHs and their derivatives determined in a large city: Correlations with their atmospheric aerosol. *Chemosph.*,
505 93, 1678-1684, 2013.
- 506 Borbély-Kiss, I., Haszpra, L., Koltay, E., László, S., Mészáros, A., Mészáros, E., and Szabó, S.: Elemental
507 concentrations and regional signatures in atmospheric aerosols over Hungary. *Physica Scripta*, 37, 299-304,
508 1988.
- 509 Ciccioli, P., Cecinato, A., Brancaleoni, E., Frattoni, M., Zacchei, P., Miguel, A., and de Castro Vasconcellos, P.:
510 Formation and transport of 2-nitrofluoranthene and 2-nitropyrene of photochemical origin in the troposphere.
511 *J. Geophys. Res.*, 101, 19567-19582, 1996.
- 512 Claxton, L.D., Matthews, P.P., and Warren, S.H.: The genotoxicity of ambient outdoor air, a review: Salmonella
513 mutagenicity. *Mutation Res. Rev.* 567, 347-399, 2004.
- 514 Degrendele, C., Audy, O., Hofman, J., Kučerik, J., Kukučka, P., Mulder, M.D., Příbylová, P., Prokeš, R., Šaňka,
515 M., Schaumann, G.E., and Lammel, G.: Diurnal variations of air-soil exchange of semi-volatile organic
516 compounds (PAHs, PCBs, OCPs and PBDEs) in a central European receptor area. *Environ. Sci. Technol.*, 50,
517 4278-4288, 2016.
- 518 Draxler, R.R., and Rolph, G.D.: HYSPLIT (HYbrid Single-Particle Lagrangian Integrated Trajectory) Model
519 access via NOAA ARL READY. NOAA Air Resources Laboratory, Silver Springs, USA. 2003, Available from:
520 <http://www.arl.noaa.gov/ready/hysplit4.html>.
- 521 EEA: European emission inventory report 1990-2012 under the UNECE Convention on Long-range Transboundary
522 Air Pollution (LRTAP), European Environment Agency Technical Report No. 12/2014, Copenhagen, 2014, 132
523 pp.
- 524 EMEP: Transboundary particulate matter, photo-oxidants, acidifying and eutrophying components. Co-operative
525 Programme for Monitoring and Evaluation of the Long-range Transmission of Air Pollutants in Europe, EMEP
526 Report No. 1/2015, Oslo, 150+78 pp. Available from:
527 http://emep.int/publ/reports/2015/EMEP_Status_Report_1_2015.pdf, 2015
- 528 Endo, S., and Goss, K.U.: Applications of poly-parameter linear free energy relationships in environmental
529 chemistry. *Environ. Sci. Technol.*, 48, 12477-12491, 2014.
- 530 Fan, Z.H., Kamens, R.M., Hu, J.X., Zhang, J.B., and McDow, S.: Photostability of nitr-polycyclic aromatic
531 hydrocarbons on combustion soot particles in sunlight. *Environ. Sci. Technol.*, 30, 1358-1364, 1996.
- 532 Feilberg, A., and Nielsen, T.: Effect of aerosol chemical composition on the photodegradation of nitro-PAHs.
533 *Environ. Sci. Technol.*, 34, 789-797, 2000.
- 534 Feilberg, A., and Nielsen, T.: Photodegradation of nitro-PAHs in viscous organic media used as models of organic
535 aerosols. *Environ. Sci. Technol.*, 35, 108-113, 2001.
- 536 Feilberg, A., Poulsen, M.W.B., Nielsen, T., and Skov, H.: Occurrence and sources of particulate nitro polycyclic
537 aromatic hydrocarbon in ambient air in Denmark. *Atmos. Environ.*, 35, 353-366, 2001.
- 538 Finizio, A., Mackay, D., Bidleman, T., and Harner, T.: Octanol-air partition coefficient as a predictor of
539 partitioning of semi-volatile organic chemicals to aerosols. *Atmos. Environ.*, 31, 2289-2296, 1997.



- 540 Finlayson-Pitts, B.J., and Pitts, J.N.: Chemistry of the Upper and Lower Atmosphere: Theory, Experiments,
541 Application, San Diego (Academic Press), USA, 2000
- 542 García-Berrios, Z.I., Arce, R., Burgos-Martínez, M., and Burgos-Polanco, N.D.: Phototransformations of
543 environmental contaminants in models of the aerosol: 2 and 4-nitropyrene. *J. Photochem. Photobiol. A*, 332,
544 131-140, 2017.
- 545 Garner, R.C., Stanton, C.A., Martin, C.N., Chow, F.L., Thomas, W., Hübner, D., and Herrmann, R.: Bacterial
546 mutagenicity and chemical analysis of polycyclic aromatic hydrocarbons and some nitro derivatives in
547 environmental samples collected in West Germany. *Environ Mutagen*, 8, 109-117, 1986.
- 548 Goss, K.U.: Predicting the equilibrium partitioning of organic compounds using just one linear solvation energy
549 relationship (LSER). *Fluid Phase Equilib.*, 233, 19-22, 2005.
- 550 Goss, K.U., and Schwarzenbach, R.P.: Linear free energy relationships used to evaluate equilibrium partitioning
551 of organic compounds. *Environ. Sci. Technol.*, 35, 1-9, 2001.
- 552 Grosjean, D., Fung, K., and Harrison, J.: Interactions of polycyclic aromatic hydrocarbons with atmospheric
553 pollutants. *Environ. Sci. Technol.*, 17, 673-679, 1983.
- 554 Halsall, C.J., Sweetman, A.J., Barrie, L.A., and Jones, K.C.: Modelling the behaviour of PAHs during
555 atmospheric transport from the United Kingdom to the Arctic. *Atmos. Environ.* 35, 255-267.
- 556 Hayakawa, K. (2016) Environmental behaviors and toxicities of polycyclic aromatic hydrocarbons and
557 nitropolycyclic aromatic hydrocarbons. *Chem. Pharm. Bull.*, 64, 83-94, 2001.
- 558 Inomata, S., Fushimi, A., Sato, K., Fujitani, Y., and Yamada, H.: 4-Nitrophenol, 1-nitropyrene, and 9-
559 nitroanthracene emissions in exhaust particles from diesel vehicles with different exhaust gas treatments.
560 *Atmos. Environ.*, 110, 93-102, 2015.
- 561 Jaenicke, R.: Aerosol physics and chemistry. *Landolt-Börnstein Neue Serie b*, 4, 391-457, 1988.
- 562 Jariyasopit, N., Zimmermann, K., Schrlau, J., Arey, J., Atkinson, R., Yu, T.W., Dashwood, R.H., Tao, S., and
563 Massey Simonich, S.L.: Novel NPAH formation from heterogeneous reactions of PAHs with NO₂, NO₃/N₂O₅,
564 OH radicals, and OH radicals: Prediction, laboratory studies and mutagenicity. *Environ. Sci. Technol.*, 48,
565 412-419, 2014a.
- 566 Jariyasopit, N., Zimmermann, K., Schrlau, J., Arey, J., Atkinson, R., Yu, T.W., Dashwood, R.H., Tao, S., and
567 Massey Simonich, S.L.: Heterogeneous reactions of particulate matter-bound PAHs and NPAHs with
568 NO₃/N₂O₅, OH radicals, and O₃ under simulated long-range atmospheric transport conditions: Reactivity and
569 mutagenicity. *Environ. Sci. Technol.*, 48, 10155-10164, 2014b.
- 570 Keyte, I.J., Harrison, R.M., and Lammel, G.: Chemical reactivity and long-range transport potential of polycyclic
571 aromatic hydrocarbons – a review. *Chem. Soc. Rev.*, 42, 9333-9391, 2013.
- 572 Keyte, I.J., Albinet, A., and Harrison, R.M.: On-road traffic emissions of polycyclic aromatic hydrocarbons and
573 their oxy- and nitro- derivative compounds measured in road tunnel environments. *Sci. Total Environ.*, 566-
574 567, 1131-1142, 2016.
- 575 Kouvarakis, G., Tsigaridis, K., Kanakidou, M., and Mihalopoulos, N.: Temporal variations of surface regional
576 background ozone over Crete Island in the Southeast Mediterranean. *J. Geophys. Res.*, 105, 4399-4407, 2000.
- 577 Lafontaine, S., Schrlau, J., Butler, J., Jia, Y.L., Harper, B., Harris, S., Bramer, L.M., Waters, K.M., Harding, A.,
578 and Massey Simonich, S.L.: Relative influence of trans-Pacific and regional atmospheric transport of PAHs in
579 the Pacific Northwest, U.S. *Environ. Sci. Technol.*, 49, 13807-13816, 2015.
- 580 Lammel, G., Audy, O., Besis, A., Efstathiou, C., Eleftheriadis, K., Kohoutek, J., Kukučka, P., Mulder, M.D.,
581 Příbylová, P., Prokeš, R., Rusina, T., Samara, C., Sofuoglu, A., Sofuoglu, S.C., Taşdemir, Y., Vassilatou, V.,
582 Voutsas, D., and Vrana, B.: Air and seawater pollution and air-sea gas exchange of persistent toxic substances
583 in the Aegean Sea: spatial trends of PAHs, PCBs, OCPs and PBDEs. *Environ. Sci. Pollut. Res.*, 22, 11301-
584 11313, 2015.
- 585 Lammel, G., Meixner, F.X., Vrana, B., Efstathiou, C., Kohoutek, J., Kukučka, P., Mulder, M.D., Příbylová, P.,
586 Prokeš, R., Rusina, T.S., Song, G.Z., and Tšapakis, M.: Bi-directional air-sea exchange and accumulation of
587 POPs (PAHs, PCBs, OCPs and PBDEs) in the nocturnal marine boundary layer. *Atmos. Chem. Phys.*, 16,
588 6381-6393, 2016.
- 589 Li, W., Shen, G.F., Yuan, C.Y., Wang, C., Shen, H.Z., Jiang, H., Zhang, Y.Y., Chen, Y.C., Su, S., Lin, N., and
590 Tao, S.: The gas/particle partitioning of nitro- and oxy-polycyclic aromatic hydrocarbons in the atmosphere of
591 northern China. *Atmos. Res.*, 172-173, 66-73, 2016.
- 592 Lin, Y., Qiu, X.H., Ma, Y.Q., Ma, J., Zheng, M., and Shao, M.: Concentrations and spatial distribution of
593 polycyclic aromatic hydrocarbons (PAHs) and nitrated PAHs (NPAHs) in the atmosphere of North China, and
594 the transformation from PAHs to NPAHs. *Environ. Pollut.*, 196, 164-170, 2015.
- 595 Lohmann, R., and Lammel, G.: Adsorptive and absorptive contributions to the gas particle partitioning of
596 polycyclic aromatic hydrocarbons: State of knowledge and recommended parameterisation for modelling,
597 *Environ. Sci. Technol.*, 38, 3793-3803, 2004.



- 598 Masplet, P., Pistikopoulos, P., Beyne, S., and Mouvier, G.: Long-range transport and gas/particle distribution of
599 polycyclic aromatic hydrocarbons at a remote site in the Mediterranean sea, *Atmos. Environ.*, 22, 639-650,
600 1988.
- 601 Melymuk, L., Bohlin-Nizzetto, P., Prokeš, R., Kukučka, P., and Klánová, J.: Sampling artifacts in active air
602 sampling of semivolatile organic contaminants: Comparing theoretical and measured artifacts and evaluating
603 implications for monitoring networks. *Environ. Pollut.*, 217, 97-106, 2016.
- 604 Mihalopoulos, N., Stephanou, E., Pilitsidis, S., Kanakidou, M., and Bousquet, P.: Atmospheric aerosol
605 composition above the Eastern Mediterranean region. *Tellus B*, 49, 314-326, 1997.
- 606 Nielsen, T., Seitz, B., and Ramdahl, T.: Occurrence of nitro-PAH in the atmosphere in a rural area. *Atmos.*
607 *Environ.*, 18, 2159-2165, 1984.
- 608 Pandis, S.N., Baltensperger, U., Wolfenbarger, J.K., and Seinfeld, J.H.: Inversion of aerosol data from the
609 epiphaniometer. *J. Aerosol Sci.*, 22, 417-428, 1991.
- 610 Pankow, J.F.: Overview of the gas phase retention volume behaviour of organic compounds on polyurethane
611 foam. *Atmos. Environ.*, 23, 1107-1111, 1989.
- 612 Pitts, J.N., Arey, J., Zielinska, B., Winer, A.M., and Atkinson, R.: Determination of 2-nitro-fluoranthene and 2-
613 nitropyrene in ambient particulate organic matter: Evidence for atmospheric reactions. *Atmos. Environ.*, 19,
614 1601-1608, 1985.
- 615 Ramdahl, T., Zielinska, B., Arey, J., Atkinson, R., Winer, A.M., and Pitts, J.N.: Ubiquitous occurrence of 2-
616 nitro-fluoranthene and 2-nitropyrene in air. *Nature*, 321, 425-427, 1986.
- 617 Reisen, F., and Arey, J.: Atmospheric reactions influence seasonal PAH and nitro-PAH concentrations in the Los
618 Angeles Basin. *Environ. Sci. Technol.*, 39, 64-73, 2005.
- 619 Ringuet, J., Albinet, A., Leoz-Garziandia, E., Budzinski, H., and Villenave, E.: Reactivity of polycyclic aromatic
620 compounds (PAHs, NPAHs and OPAHs) adsorbed on natural aerosol particles exposed to atmospheric
621 oxidants. *Atmos. Environ.*, 61, 15-22, 2012.
- 622 Ringuet, J., Leoz-Garziandia, E., Budzinski, H., Villenave, E., and Albinet, A.: Particle size distribution of
623 nitrated and oxygenated polycyclic aromatic hydrocarbons (NPAHs and OPAHs) on traffic and suburban sites
624 of a European megacity: Paris (France). *Atmos. Chem. Phys.*, 12, 8877-8887, 2012b.
- 625 Ringuet, J., Albinet, A., Leoz-Garziandia, E., Budzinski, H., and Villenave, E.: Diurnal/nocturnal concentrations
626 and sources of particulate-bound PAHs, OPAHs and NPAHs at traffic and suburban sites in the region of Paris
627 (France), *Sci. Total Environ.*, 437, 297-305, 2012c.
- 628 Schauer, C., Niessner, R., and Pöschl, U.: Analysis of nitrated polycyclic aromatic hydrocarbons by liquid
629 chromatography with fluorescence and mass spectrometry detection: air particulate matter, soot, and reaction
630 product studies. *Anal. Bioanal. Chem.*, 378, 725-736, 2004.
- 631 Schuetzle, D.: Sampling of vehicle emissions for chemical analysis and biological testing. *Environ. Health*
632 *Perspect.*, 47, 65-80, 1983.
- 633 Shahpoury, P., Lammel, G., Albinet, A., Sofuoğlu, A., Dumanoğlu, Y., Sofuoğlu, S.C., Wagner, Z., and Ždimal,
634 J.: Model evaluation for gas-particle partitioning of polycyclic aromatic hydrocarbons in urban and non-urban
635 sites in Europe – Comparison between single- and poly-parameter linear free energy relationships based on a
636 multi-phase aerosol scenario. *Environ. Sci. Technol.*, 50, 12312-12319, 2016.
- 637 Stohl, A., Hitznerberger, M., and Wotawa, G.: Validation of the Lagrangian particle dispersion model
638 FLEXPART against large scale tracer experiments. *Atmos. Environ.*, 32, 4245-4264, 1998.
- 639 Stohl, A., Forster, C., Frank, A., Seibert, P., and Wotawa, G.: Technical note: The Lagrangian particle dispersion
640 model FLEXPART version 6.2. *Atmos. Chem. Phys.*, 5, 2461-2474, 2005.
- 641 Tomaz, S., Shahpoury, P., Jaffrezo, J.L., Lammel, G., Perraudin, E., Villenave, E., and Albinet, A.: One year
642 study of polycyclic aromatic compounds at an urban site in Grenoble (France): seasonal variations, gas/particle
643 partitioning and cancer risk estimation, *Sci. Total Environ.*, 565, 1071-1083, 2016.
- 644 Tsapakis, M., and Stephanou, E.G.: Diurnal cycle of PAHs, nitro-PAHs and oxy-PAHs in a high oxidant capacity
645 marine background atmosphere. *Environ. Sci. Technol.*, 41, 8011-8017, 2007.
- 646 Vincenti, M., Maurino, V., Minero, C., and Pelizzetti, E.: Determination of nitro-substituted polycyclic aromatic
647 hydrocarbons in the Antarctic airborne particulate. *Intl. J. Environ. Anal. Chem.*, 79, 257-272, 2001.
- 648 Vrekoussis, M., Liakakou, E., Kocak, M., Kubilay, N., Oikonomou, K., Sciare, J., and Mihalopoulos, N. (2005)
649 Seasonal variability of optical properties of aerosols in the Eastern Mediterranean, *Atmos. Environ.* 39, 7083-
650 7094.
- 651 Yamasaki, H., Kuwata, K., and Miyamoto, H.: Effects of ambient temperature on aspects of airborne polycyclic
652 aromatic hydrocarbons. *Environ. Sci. Technol.*, 16, 189-194, 1982.
- 653 Zimmermann, K., Atkinson, R., Arey, J., Kojima, Y., and Inazu, K.: Isomer distributions of molecular weight 247
654 and 273 nitro-PAHs in ambient samples, NIST diesel SRM, and from radical-initiated chamber reactions.
655 *Atmos. Environ.*, 55, 431-439, 2012.



- 656 Zimmermann, K., Jariyasopit, N., Massey Simonich, S.L., Tao, S., Atkinson, R., and Arey, J.: Formation of
657 NPAHs from the heterogeneous reaction of ambient particle-bound PAHs with $N_2O_5/NO_3/NO_2$. Environ. Sci.
658 Technol., 47, 8434-8442, 2013.
659



20

660 Table 1. Overview time weighted mean concentrations in the particulate and gas phases, and
 661 ambient temperature. Data subsets (B = background, P = polluted, D = day mean, N = night
 662 mean) and mass size distribution (<0.45/0.45-0.95/0.95-1.5/1.5-3.0/3.0-7.2/7.2-10 μm
 663 aerodynamic equivalent diameter) in brackets.

Site	Phase	$\Sigma_{11} 3\text{-}4\text{rNPAH}$ (pg m^{-3})	$\Sigma_6 4\text{rPAH}$ (pg m^{-3})
Marine	particulate (n = 8)	4.1 (3.5/0.6/0.2/0.03/0.03/0.00) (B: 0.2/P: 8.7)	43 (28/8.1/1.2/6.2/4.3/1.7) (B: 7.9/P: 42.4)
	gas (n = 21)	18.4 (B: 13.2/P:31.7)	403 (B:321/P:595)
	T($^{\circ}\text{C}$)	25.6 (B: 27.1/P: 22.0)	
Continental	particulate (n = 22)	24.3 (20.5/2.9/0.7/0.04/0.06/0.15) (D:13.9/N:34.6)	129 (87/28/12/0.6/0.0/0.0) (D:146/N:116)
	gas (n = 22)	34.2 (D:42.9/N:25.5)	517 (D:649/N:384)
	T($^{\circ}\text{C}$)	23.1 (D:28.8/N:17.5)	

664

665



666 Table 3. Comparison of total (g + p) concentrations in air, c_{tot} (pg/m^3), with other
 667 measurements at remote and rural sites

	1NPYR (pg/m^3)	2NFLT (pg/m^3)	2NPYR (pg/m^3)	References
background CEu summer 2013	1.1	15 ^a	1.3	this work (continental)
E Mediterranean summer 2012	0.74	8.6 ^a	2.5	this work (marine)
E Mediterranean clean summer 2012	0.21	3.8 ^a	0.92	this work (marine background ^b)
E Mediterranean clean summer 2002	-	29	21	Tsapakis and Stephanou, 2007
Ross Sea coast, Antarctica	<0.02 ^c	<0.03 ^c		Vincenti et al., 2001
Himalayas, Nepal 1991	-	-	3	Ciccioli et al., 1996
Forest Amazonia 1993	2	15	8	
Rural Northern Germany 1991	-	-	3	
Rural Denmark winter-spring 1982	9±5 ^c	-	-	Nielsen et al., 1984
Semi-rural Denmark all year 1998-99	40	97	6.3	Feilberg et al., 2001
Remote Alps 2002	2.2	-	-	Schauer et al., 2004
Rural Alps 2002	6.6	-	-	
Rural Alps ^d winter 2002-03	21	96 ^a	81	Albinet et al., 2008a
Rural Alps ^d summer 2003	4.2	28 ^a	5.7	
Rural Southern France 2004	0.6	2.6 ^a	1.6	Albinet et al., 2007

668 ^a co-eluted with 3NFLT, assuming $c_{3\text{NFLT}} = 0$

669 ^b samples No. 9, 10, 19 and 22 in Fig. S3

670 ^c particulate phase concentration only

671 ^d Val de Maurienne sites (Albinet et al., 2008a)

672



673 Table 4: Selected 4-ring PAHs and primary and secondary 3-4 ring NPAH total (g + p) time-
 674 weighted mean concentrations $\pm\sigma$ (pg m^{-3}). Potential yields, $c_{\text{NPAH}}/c_{\text{PAH}}$, in brackets. σ given
 675 for $n > 2$.

Site		Marine			Continental
Data subset		all ($n = 8^a$)	marine background ($n = 2^b$)	background with urban influence ($n = 2^c$)	all ($n = 22$)
Primary	FLT	213 \pm 161	161	259	342 \pm 215
	PYR	146 \pm 130	103	188	226 \pm 131
Primary and secondary (potential yield)	2NFLN ^d	0.038 \pm 0.12	<0.18	0.15	0.034 \pm 0.044
	1NPYR	0.62 \pm 1.1 (0.4 \pm 0.2%)	0.21 (0.2%)	1.4 (0.7%)	1.1 \pm 0.6 (0.6 \pm 0.3%)
Secondary (yield)	2NFLT ^e	7.7 \pm 8.5 (3.6 \pm 2.0%)	1.68 (1.0%)	11.0 (4.2%)	15 \pm 10 (6.5 \pm 7.5%)
	2NPYR	2.2 \pm 2.6 (1.5 \pm 0.7%)	0.92 (0.9%)	3.3 (1.8%)	1.3 \pm 1.7 (0.74 \pm 1.09%)

676 ^a 8 filter and 21 PUF samples

677 ^b 2 filter and 6 PUF samples i.e., No. 9-10 and 19-22 in Fig. S3 (urban fractional dose $D_u =$
 678 0.4%)

679 ^c 2 filter and 5 PUF sample i.e., No. 1-2 and 15-18 in Fig. S3 ($D_u = 3.1\%$)

680 ^d no yield given as c_{FLN} not quantified

681 ^e co-eluted with 3NFLT, assuming $c_{3\text{NFLT}} = 0$

682



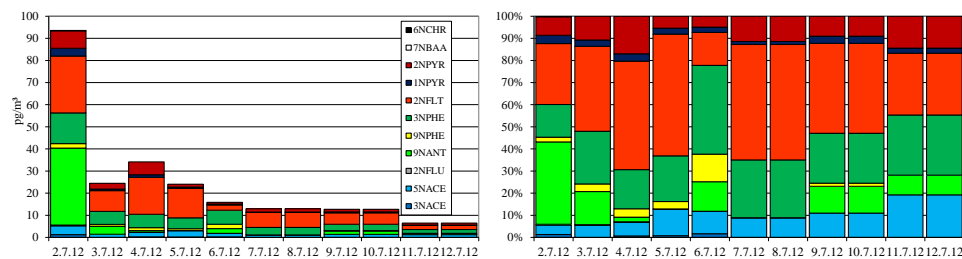
23

683 Fig. 1: Time series of absolute (a, c; pg m^{-3}) and relative (b, d) total (gas + particulate) NPAH
684 concentrations at the (a, b) marine (24 h means shown^a) and (c, d) continental site (day / night
685 means)

686

a.

b.

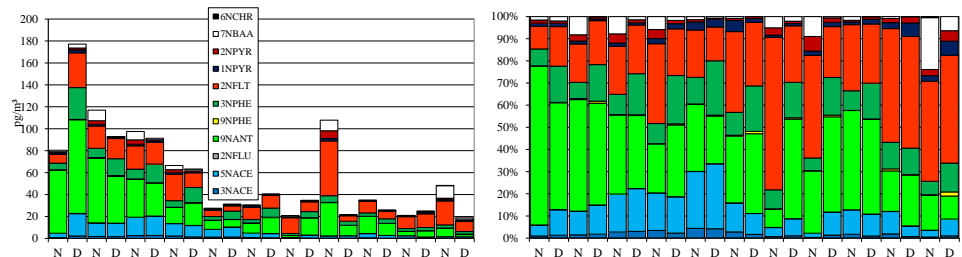


687

688

c.

d.



689

690 ^a gas-phase (PUF) sampled day / night, particulate phase (filter) sampled 1-4 subsequent days /
691 nights, 4 during the period 7.-12.7.12

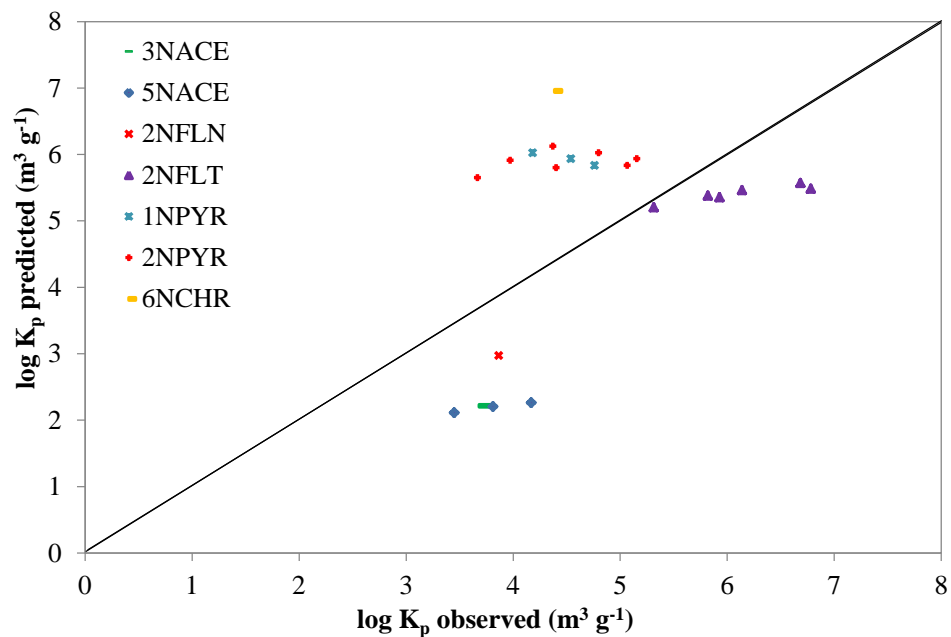
692



24

693 Fig. 2: Predicted versus experimental $\log K_p$ ($\text{m}^3 \text{air g}^{-1} \text{PM}$) for NPAHs using the multi-phase
694 ppLFER model at the (a) marine and (b) continental site

695 a.

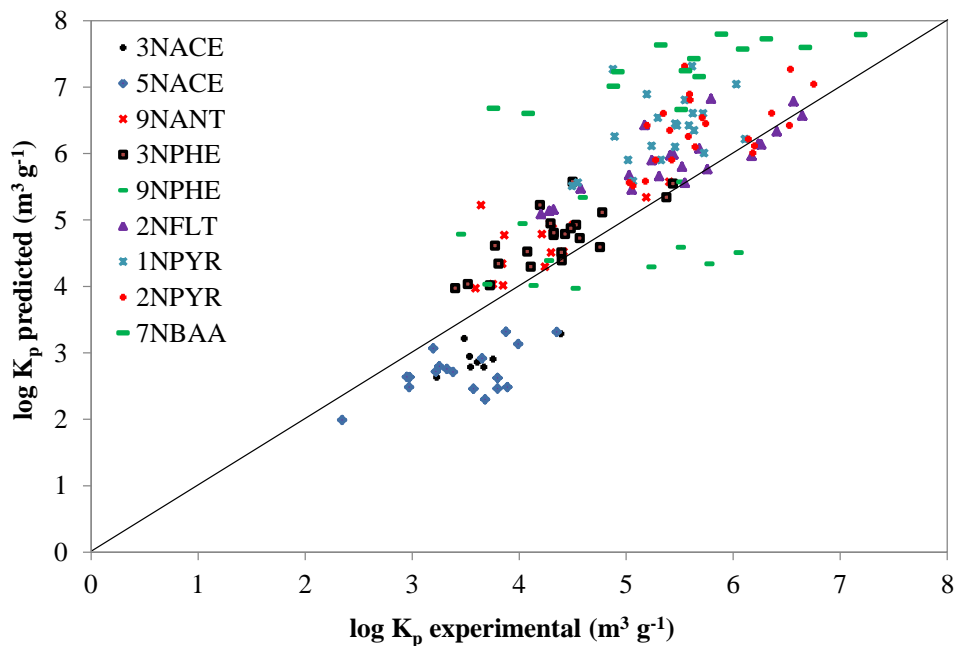


696

697 b.



25



698
699
700



701 Fig. 3. Time-weighted mean Σ_6 4rPAH and Σ_{11} 3-4rNPAH mass size distributions (%) at the
702 marine and continental sites. Upper cut-off of impactor stage given in μm of aerodynamic
703 particle size.

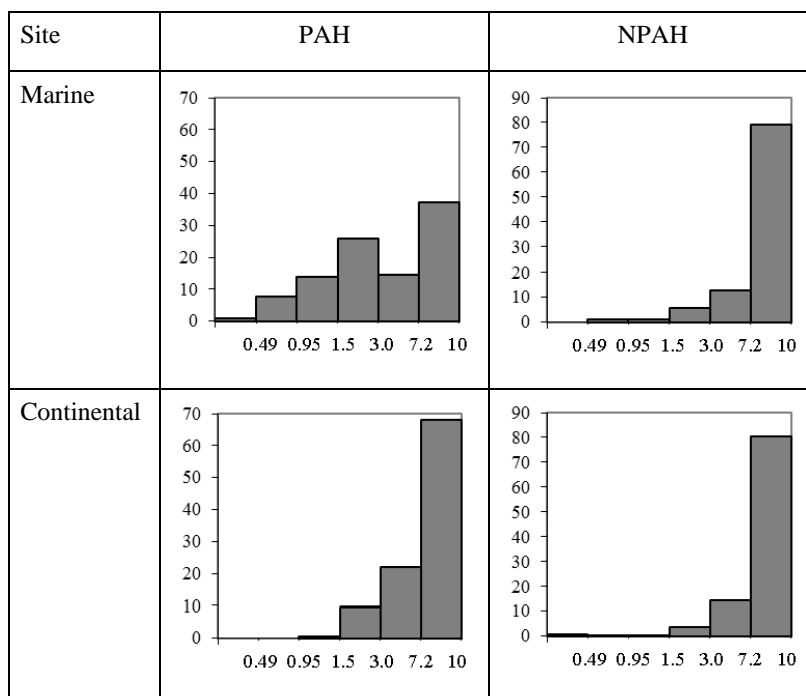




Table 2. Total (g + p) time-weighted concentrations, c_{tot} (pg m^{-3}), particulate mass fraction, $\theta = c_p / c_{\text{tot}}$, and mass median diameter (MMD, μm), of 2-4-ring NPAHs and 4-ring PAHs at the marine (as 'mean (background mean/ urban influence mean)', $n = 8(2^a/2^b)$) and continental (as 'mean (day mean/ night mean)', $n = 22(11/11)$) sites, together with temperature and supporting aerosol parameters (PM_{10} and carbonaceous mass fractions). LOQ = limit of quantification, nd = no data.

	Marine			Continental		
	c_{tot} (pg m^{-3})	θ	MMD (μm)	c_{tot} (pg m^{-3})	θ	MMD (μm)
FLT	226 (161/259)	0.07 (0.03/0.08)	0.58 (0.43/0.52)	342 (432/251)	0.11 (0.11/0.12)	0.062 (0.101/0.034)
PYR	158 (103/188)	0.04 (0.01/0.06)	0.21 (0.022/0.22)	226 (276/176)	0.18 (0.18/0.19)	0.075 (0.105/0.055)
BBN	4.1 (2.0/5.5)	0.01 (nd/0.06)	0.022 (nd/0.022)	15 (16/13)	0.61 (0.58/0.65)	0.079 (0.127/0.053)
BAA	2.8 (<LOQ/3.4)	0.28 (nd/0.35)	0.022 (nd/0.022)	16 (14/18)	0.91 (0.90/0.92)	0.070 (0.090/0.060)
TPH	12 (8.5/14)	0.02 (nd/0.06)	0.022 (nd/0.022)	23 (26/21)	0.51 (0.41/0.63)	0.070 (0.090/0.057)
CHR	23 (10/29)	0.22 (0.09/0.25)	0.15 (0.022/0.15)	41 (44/38)	0.75 (0.71/0.80)	0.074 (0.105/0.055)
Σ_6 4rPAH	426 (284/499)	0.07 (0.02/0.07)	0.31 (0.19/0.28)	663 (808/517)	0.21 (0.19/0.25)	0.071 (0.10/0.051)
3NACE	0.21 (0.17/0.39)	0.05 (0.00/0.19)	0.022 (nd/0.022)	1.0(1.0/1.0)	0.05 (0.01/0.11)	0.022 (nd/0.022)
5NACE	1.8 (1.5/2.0)	0.07 (0.00/0.00)	0.022 (nd/nd)	6.8 (7.6/6.0)	0.03 (0.01/0.05)	0.022 (0.022/0.022)
2NFLN	0.01 (<LOQ/0.15)	0.02 (nd/0.00)	1.19 (nd/nd)	0.035 (0.035/0.034)	0.00 (0.00/0.00)	nd
9NPHE	0.73 (0.84/0.55)	0.00 (0.00/0.00)	nd	0.21 (0.28/0.13)	0.36 (0.43/0.20)	0.022 (0.022/nd)



3NPHE	4.8 (3.4/5.0)	0.00 (nd/nd)	nd	7.4 (10.0/4.8)	0.24 (0.15/0.44)	0.109 (0.067/0.116)
9NANT	4.2 (1.1/8.2)	0.00 (0.00/0.00)	nd	22 (22/22)	0.23 (0.14/0.33)	0.022 (0.022/0.022)
2NFLT ^c	8.6 (3.8/11)	0.32 (nd/0.48)	0.040 (nd/0.080)	15 (13/18)	0.78 (0.54/0.95)	0.054 (0.035/0.050)
1NPYR	0.75 (0.21/1.4)	0.33 (0.00/0.61)	0.061 (nd/0.14)	1.1 (1.1/1.2)	0.82 (0.76/0.88)	0.030 (0.031/0.029)
2NPYR	2.5 (0.92/3.3)	0.53 (0.19/0.70)	0.058 (0.060/0.055)	1.3 (0.73/2.0)	0.93 (0.83/0.97)	0.070 (0.040/0.061)
7NBAA	<LOQ	nd	nd	2.5 (0.77/4.2)	0.91 (0.56/0.97)	0.074 (0.038/0.057)
6NCHR	0.02 (<LOQ/0.07)	1.00 (nd/1.00)	2.12 (nd/2.12)	0.01 (<LOQ/0.02)	1.00 (nd/1.00)	0.022 (nd/0.022)
Σ _{11,3} - 4rNPAH	23.7 (11.8/32.0)	0.22 (0.01/0.21)	0.34(0.33/0.34)	58 (56/59)	0.16 (0.13/0.17)	0.039 (0.036/0.040)
PM ₁₀ (µg/m ³)	34.9 (21.0/55.5)		0.58 (1.13/0.62)	22.1 (19.5/24.5)		nd
EC (µg/m ³)	0.11 (0.09/0.17)		0.03(0.05/0.03)	0.31 (0.28/0.33)		0.21(0.19/0.22)
OC (µg/m ³)	1.9 (1.5/3.0)		0.17(0.16/0.15)	3.6 (3.3/3.9)		0.16(0.13/0.18)
T (°C)		25.6 (27.0/22.2)			23.1 (28.8/17.5)	

^a 2 filter and 4 PUF samples i.e., No. 9, 10, 19 and 22 in Fig. S3

^b 1 filter and 1 PUF sample i.e., No. 1 and 2 in Fig. S3

^c co-eluted with 3NFLT, assuming c_{3NFLT} = 0